Pergamon

Cement and Concrete Research 31 (2001) 1075–1085

CEMENT AND CONCRETE RESEARCH

Shrinkage-reducing admixtures and early-age desiccation in cement pastes and mortars

D.P. Bentz[a,*], M.R. Geiker[b], K.K. Hansen[b]

[a]*Building and Fire Research Laboratory, National Institute of Standards and Technology, 100 Bureau Drive Stop 8621, Gaithersburg, MD 20899-8621, USA*
[b]*Technical University of Denmark, Building 118, DK-2800 Lyngby, Denmark*

Received 3 January 2001; accepted 9 April 2001

Abstract

Fundamental studies of the early-age desiccation of cement-based materials with and without a shrinkage-reducing admixture (SRA) have been performed. Studies have been conducted under both sealed and drying conditions. Physical measurements include mass loss, surface tension, X-ray absorption to map the drying profile, internal relative humidity (RH), and autogenous deformation. Interestingly, although the SRA accelerates the drying of bulk solutions, in cement paste with a water-to-cement (w/c) ratio of 0.35, it actually reduces the measured drying rate. Based on the accompanying X-ray absorption measurements and a simple three-dimensional microstructure model, an explanation for this observation is proposed. In sealed systems, at equivalent hydration times, the SRA maintains a greater internal RH and reduces the induced autogenous deformation. Thus, these admixtures should be beneficial to low w/c ratio concretes undergoing self-desiccation, in addition to their normal usage to reduce drying shrinkage.

Keywords: Cement paste; Drying; Humidity; Shrinkage; Surface tension

1. Introduction

Despite the best efforts to avoid it, in practice, most concretes crack. The cracking can be due to a variety of causes including thermal gradients, moisture gradients, and attack by the external or internal environment (sulfate attack, alkali–silica reaction, etc.). The failure of concrete due to cracking typically follows the classic bathtub service life function [1], with significant early-age cracking. Concrete that survives this early-age period in a crack-free condition may remain so for decades before cracking due to the above-mentioned degradation mechanisms. Clearly, avoiding early-age cracking is often critical to providing concrete that meets its intended design purpose and performs acceptably throughout its intended service life.

In low water-to-cement (w/c) ratio concretes, one significant contributor to early-age cracking is the self-desiccation [2] and autogenous deformation that occurs during the early-age period. As the cement hydrates, the reaction products occupy less space than the reactants (Le Chatelier contraction/chemical shrinkage). This chemical shrinkage results in a self-desiccation and the creation of empty porosity within the material (once set has occurred). The menisci present at the interfaces between the water-filled and empty pores will result in the development of stresses within the liquid phase that will also, of course, result in autogenous stresses and strains within the solid framework of the hydrating cement paste. Because the stresses in the pore solution are directly proportional to its surface tension, it seems logical that shrinkage-reducing admixtures (SRA — conventionally used to control drying shrinkage) [3], which lower this surface tension, could also be used to mitigate autogenous shrinkage and thus early-age cracking in low w/c ratio cement-based materials. In this paper, fundamental studies on the influence of SRAs on desiccation in cement pastes and mortars cured under sealed and drying conditions will be presented.

2. Experimental

Studies have been conducted on three different systems: (1) bulk liquids, (2) cement pastes, and (3) mortars. For the bulk liquids, the properties of distilled water were contrasted

* Corresponding author. Tel.: +1-301-975-5865; fax: +1-301-990-6891.
E-mail address: dale.bentz@nist.gov (D.P. Bentz).

0008-8846/01/$ – see front matter
PII: S0008-8846(01)00519-1

against a solution prepared by adding 6% by mass of Eclipse SRA[1] to distilled water. The surface tensions of the two solutions were measured at 23°C (and 55% RH) using a Dunouy tensiometer. In addition, mass loss measurements were made for the solutions placed in parallelepiped cuvettes $10 \times 10 \times 5$ mm^3 deep, open at one end. These cuvettes were exposed to a constant environment of approximately 25°C and 50% RH.

Two cements were used for the cement paste studies. Mass loss measurements and concurrent X-ray absorption measurements to determine the drying profiles [4–6] were performed for cement pastes with a w/c ratio of 0.35, prepared using a low-alkali sulfate-resistant Aalborg Portland cement. The cement has a Blaine fineness of 368 m^2/kg and a Bogue calculated phase composition of 58% C_3S, 25% C_2S, 4.0% C_3A, and 7.3% C_4AF, with a 3.4% calcium sulfate content. Pastes were prepared with distilled water, and with and without a 2% mass addition (by mass of cement) of the SRA. The pastes were mixed by hand and placed in cuvettes. Drying kinetics were monitored both in the lab and in the X-ray environmental chamber (a slightly more severe drying environment due to the air circulation within the chamber). In addition to the two ''pure'' systems, two composite layered systems were also prepared. Both layerings, paste with the SRA over paste without the SRA and vice versa, were examined in this study.

For a second experiment, cement paste specimens were prepared from an ultrafine cement with a Blaine fineness of 654 m^2/kg. This cement's potential Bogue composition was 73.5% C_3S, 16.5% C_2S, 7.1% C_3A, and 2.5% C_4AF. Cement pastes with a w/c = 0.3, with and without a 2% mass addition of the SRA, were mixed by hand. The internal relative humidity (RH) of these pastes under sealed curing conditions at 25°C was monitored for 11 days using a Rotronic Hygroscope DT equipped with four measuring cells [7]. Before and after this experimental run, the Rotronic equipment was calibrated using salt solutions with RHs between 75% and 100%. For companion specimens, the maximum standard deviation in RH between readings was 0.42%, with an average standard deviation of 0.17%. After 11 days of sealed curing, the nonevaporable water contents of the specimens were determined by loss on ignition (mass at 1050°C vs. mass at 105°C). The measured values were corrected for the loss on ignition of the cement powder. For the specimens with the SRA, the results were further corrected by 0.02 to account for the 2% addition of organic SRA (boiling point of about 212°C).

Finally, mortars were prepared using the low-alkali Portland cement with a water-to-solid binder (w/s — where binder is cement + silica fume) ratio of 0.35 and an 8% replacement of cement by silica fume (mass basis). The silica fume used had a specific surface area of 23.2 m^2/g. Once again, mortars with and without 2% addition of the SRA were prepared by mixing in a 5-l epicyclic mixer. For these mortars prepared with CEN standard sand EN 196-1, the following measurements were performed: cylinder compressive strength after 7 and 28 days of sealed curing, internal RH development over the course of at least 21 days, and autogenous deformation using a custom-built dilatometer immersed in a constant temperature oil bath [8,9]. After setting was achieved, the maximum standard deviation in relative deformation (dilatometer) readings made on companion specimens was 27 microstrains, with typical standard deviations being in the range of 5–17 microstrains. For this portion of the study, all curing and measurements were conducted at a temperature of 30°C under sealed conditions.

3. Results and discussion

Five readings of the surface tension were performed for each of the two liquids. For distilled water, the mean value of the measured surface tension was 0.0765 N/m with a standard deviation of 0.0003 N/m. For the solution containing 6% SRA, the mean value was 0.0325 N/m with a standard deviation of 0.0005 N/m, a reduction of about 57%.

It might also be expected that the lower surface tension would result in a greater drying rate for the bulk solution containing the SRA [10]. This hypothesis is confirmed in the results presented in Fig. 1, which plots the cumulative mass loss for the two solutions, as well as for the organic SRA itself. The *initial* mass loss is substantially greater for the solution containing the SRA than for distilled water. Naturally, one might expect that the same trend would be observed in cement pastes, i.e., cement pastes with the SRA will dry at a faster rate than those without it. But, is this indeed observed . . .?

In fact, the exact opposite behavior is observed in the cement paste specimens examined in this study, as shown in the mass loss curves presented in Fig. 2. Here, relative water mass loss indicates the fraction of the water initially present in the specimen that has been removed due to drying. Clearly, the presence of the SRA is now reducing the mass loss rate. Some insight into why this is the case is provided in the concurrent X-ray absorption results. The results plotted in Figs. 3 and 4 show the differences in X-ray counts over time, relative to the setting time of about 3 h. This count difference is plotted against the location sampled by the X-ray system, with the bottom of the specimens being located at position 0 mm and the top exposed surface at 8 mm. As the cement paste dries out, the X-ray counts increase (resulting in a positive difference relative to any earlier time), as there is less material to absorb the X-rays passing through the specimen. The main changes in the X-ray transmission are due to water movement, as little change

[1] Certain materials and commercial equipment are identified in this paper to specify the experimental procedure. In no case does such identification imply endorsement by the National Institute of Standards and Technology, nor does it indicate that the products are necessarily the best available for the purpose.

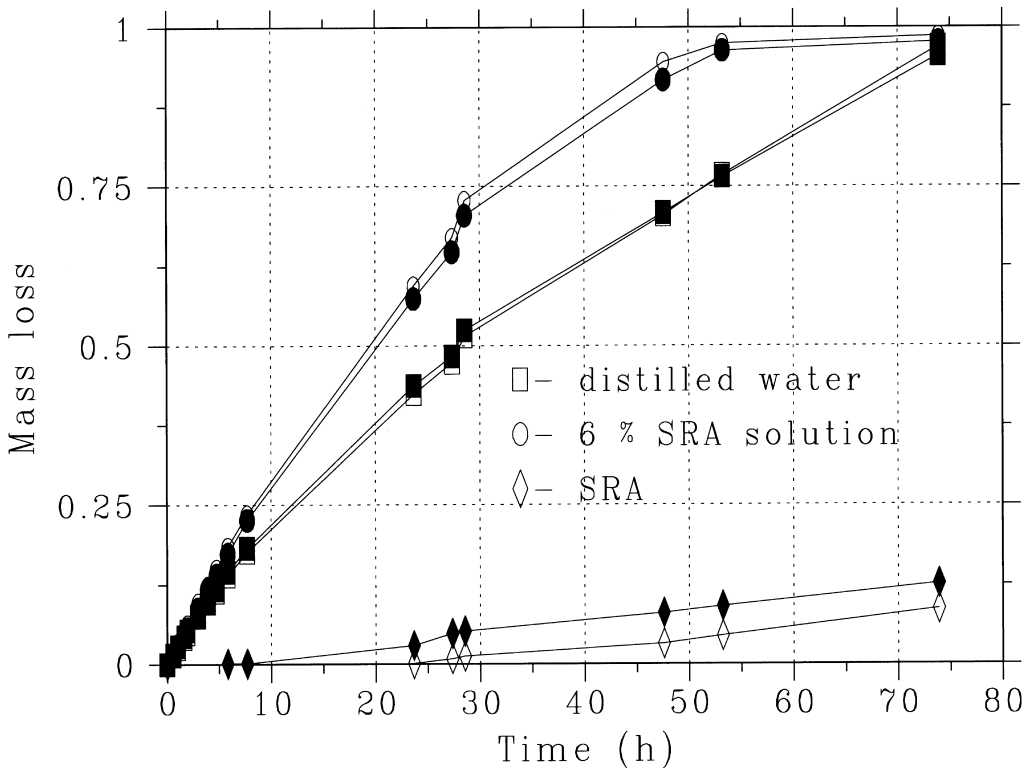

Fig. 1. Mass loss of bulk solutions vs. time. Filled and hollow data points indicate the two replicates examined for each of the three solutions.

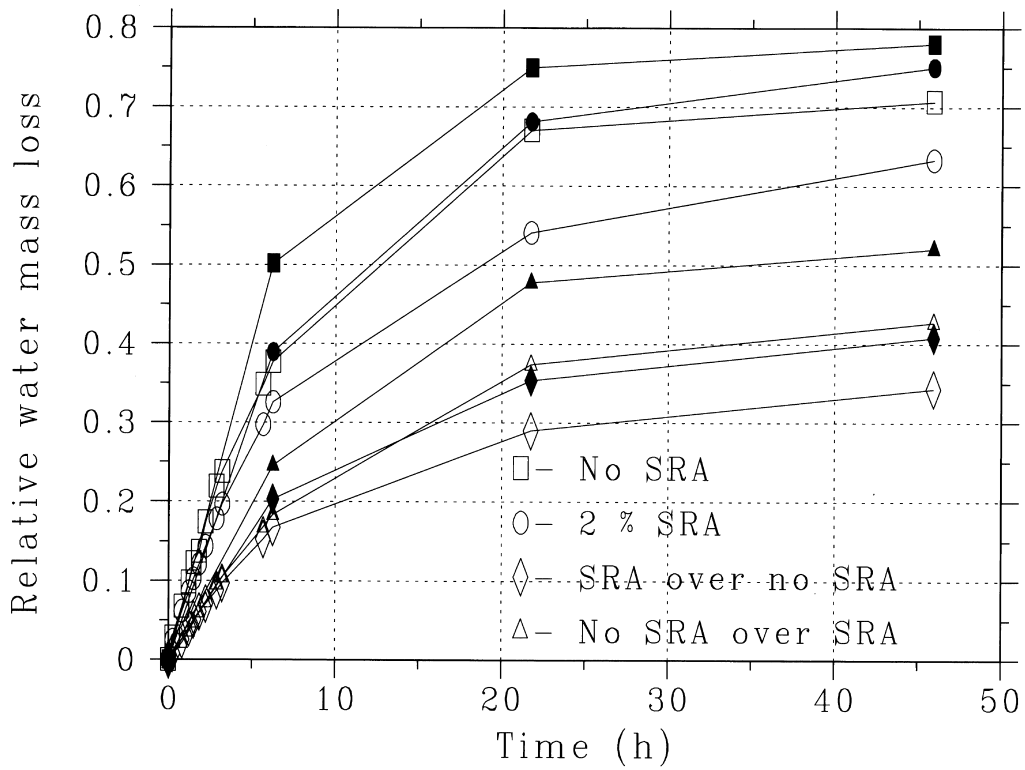

Fig. 2. Mass loss of cement paste specimens (w/c = 0.35) vs. time. Filled data points correspond to specimens exposed in the X-ray environmental chamber and hollow data points to those exposed in the laboratory.

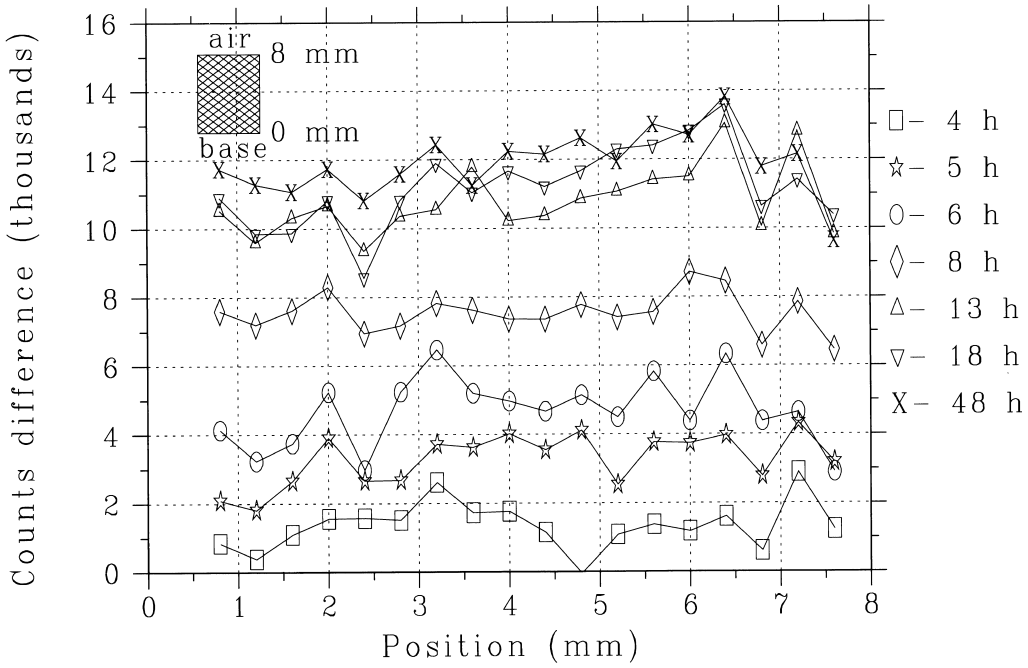

Fig. 3. Differences in normalized X-ray counts vs. position for w/c = 0.35 cement paste without the SRA. Differences are relative to readings at 3 h.

is observed to occur during hydration under sealed conditions [5,6]. As has been observed previously [5,6], for the paste without the SRA (Fig. 3), a uniform drying is observed, with the largest pores throughout the paste thickness emptying first, followed by the next largest, etc. However, for the paste with the SRA (Fig. 4), instead of drying uniformly, at early times, a relatively sharp drying front is formed at the exposed surface of the sample. It is hypothesized that the initial drying at the surface concentrates the SRA within the remaining surface pore solution so that it is more likely to continue to dry out as opposed to "drawing" water from the higher surface tension pore solution beneath it. After 13 h or so of drying, this front begins to disappear and ultimately, a uniform drying profile is achieved.

Further insight into why the two systems exhibit different drying rates can be obtained from a simple three-dimensional microstructure model [11]. An initial three-dimen-

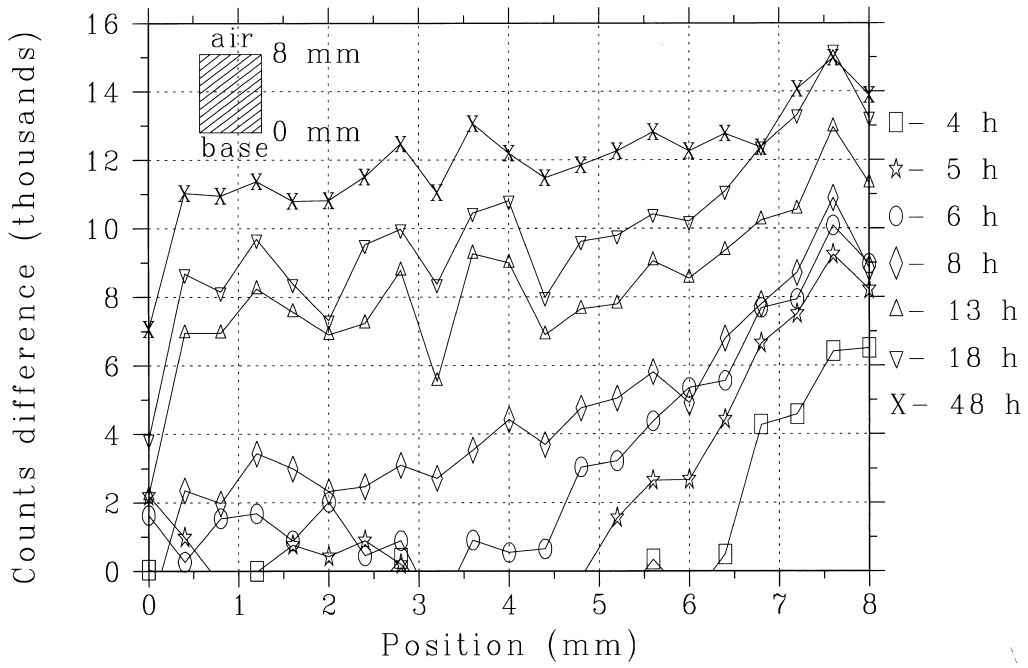

Fig. 4. Differences in normalized X-ray counts vs. position for w/c = 0.35 cement paste with the SRA. Differences are relative to readings at 3 h.

sional microstructure ($100 \times 100 \times 100$ μm^3) consisting of digitized nonoverlapping spherical particles (minimum diameter of 3 pixels; 3 μm) dispersed in water (w/c = 0.35) was created. Empty pores were then created under two conditions: (1) empty porosity was created anywhere within the microstructure by emptying the largest (spherical) pores first regardless of their location and (2) empty porosity was created by emptying the largest pores from the top surface inward to simulate the presence of a sharp drying front. Two-dimensional images from these three-dimensional microstructures are provided in Figs. 5 and 6. In the latter case, one can easily suppose that the drying rate would be reduced by the presence of a "boundary" layer at the top surface of the specimen. Water molecules that evaporate must first diffuse through this tortuous boundary layer before reaching the external environment, resulting in a reduced mass transfer coefficient. In the former case, because water is quickly and easily "rearranged" throughout the microstructure (due to its high permeability), no boundary layer is observed to form at the top surface. Here, the drying rate can remain relatively high as water molecules evaporate directly from the surface into the external environment during an extended constant rate drying period [12]. Indeed, in Fig. 2, it is observed that the drying rates for the two systems are similar for the first few hours and then diverge substantially as the paste with the SRA enters its "decreasing rate drying period" [12] well before the paste without the SRA. More details on the influence of microstructure on the constant rate and decreasing rate drying periods in porous materials can be found in the recent publication of Coussot [12]. It should be noted that for higher w/c ratio systems, if a layer of bleed water forms at the specimen surface (due to settling, etc.), it would then be expected that the drying rates would be controlled by the evaporation kinetics of the bulk solutions; in this case, the SRA might still accelerate the drying process, at least until the removal of solution from the settled microstructure is initiated.

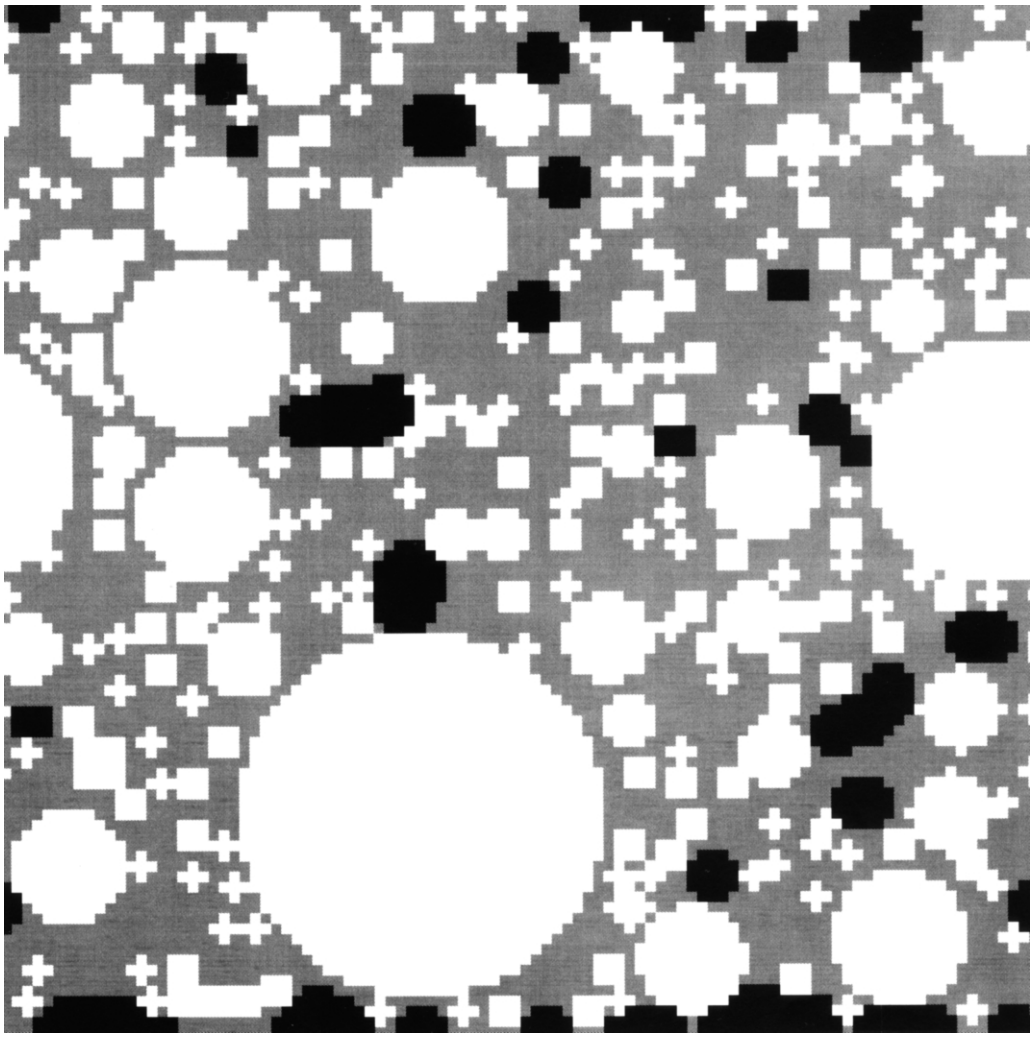

Fig. 5. Two-dimensional image from three-dimensional microstructure for the case of uniform drying. White represents the solid particles, grey water, and black empty pore space. Image is 100×100 μm^2.

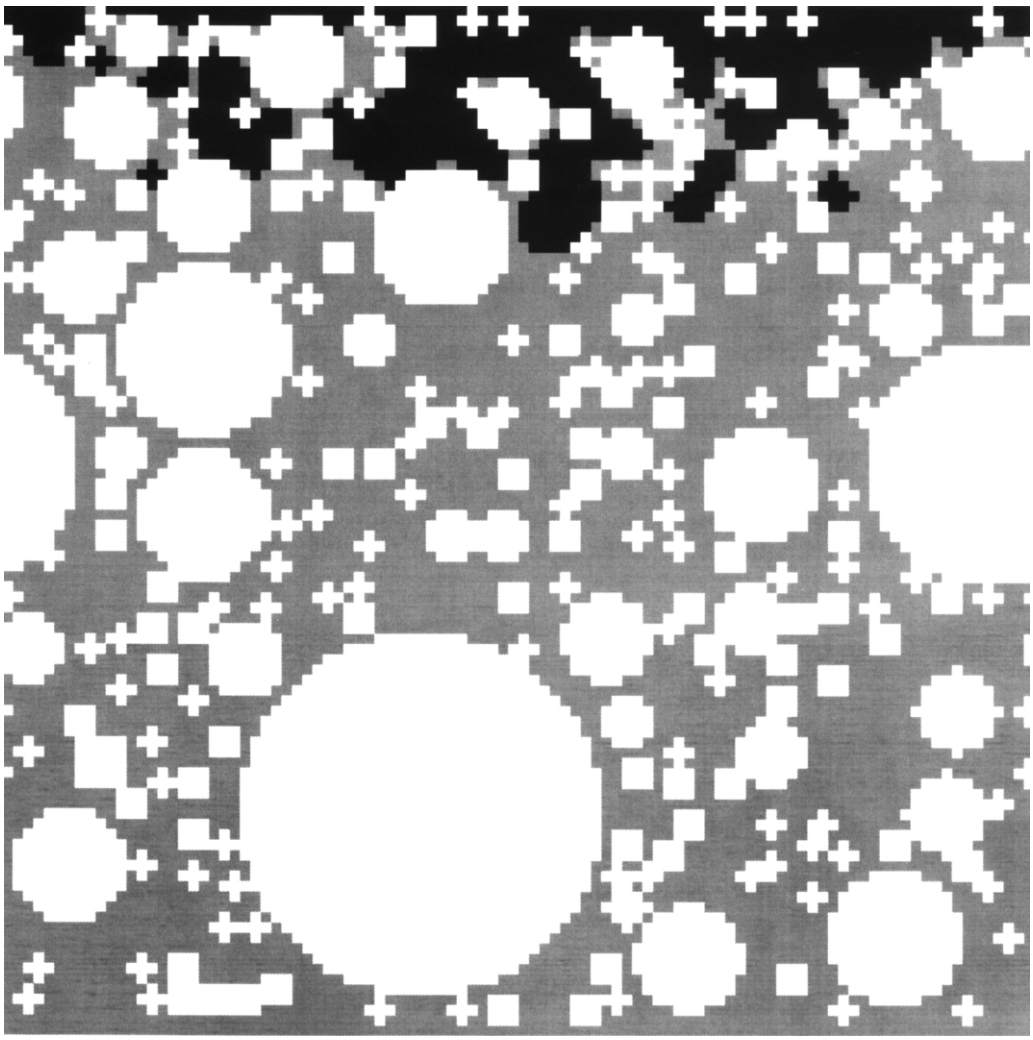

Fig. 6. Two-dimensional image from three-dimensional microstructure for the case of drying from the top surface inward. White represents the solid particles, grey water, and black empty pore space. Image is 100×100 μm^2.

It is also of interest to examine the drying kinetics and profiles for layered composite systems. The mass loss measurements for both possible geometric configurations were provided in Fig. 2. The drying profiles for the case of paste with the SRA on top of paste without the SRA and vice versa are provided in Figs. 7 and 8, respectively. When the paste containing the SRA is placed on top and exposed directly to the drying environment, it is seen to function as a very effective curing layer, significantly reducing the bulk mass loss from the specimen (Fig. 2), and particularly minimizing the water loss from the paste without the SRA that comprises the bottom layer of the system shown in Fig. 7. During the early hydration, in addition to the water loss from its top surface, the SRA paste also contributes water to the curing of the no SRA paste underneath it, as evidenced by the negative counts difference values for positions between 0 and 10 mm and times up to 13 h in Fig. 7. The higher surface tension in the pore solution in the no SRA paste allows it to "pull" water from the lower surface tension pore solution in the layer above to replace that "lost" due to chemical shrinkage and self-desiccation. Of course, as the water is pulled from the top layer to the bottom one, some of the SRA will be pulled along with it. This is indicated by the "drying front" progressing deeper and deeper into the composite specimen at longer drying times (>8 h). Perhaps this preferential water movement due to surface tension differences can be used to advantage in the design of future curing systems and methodologies.

When the paste without the SRA comprises the top layer of the composite, it first pulls water from the layer underneath it and later (13 h) dries out itself, ultimately resulting in a rather uniform drying profile, as shown in Fig. 8. Similar behavior has been observed previously [5,6] for layered pastes where either the w/c ratio or the particle size distribution (PSD) of the cement varied between the two layers. In those cases, water was always observed to move preferentially from the coarse pore structure to the finer one. Here, preferential water movement is observed from the lower surface tension pore solution to the higher one.

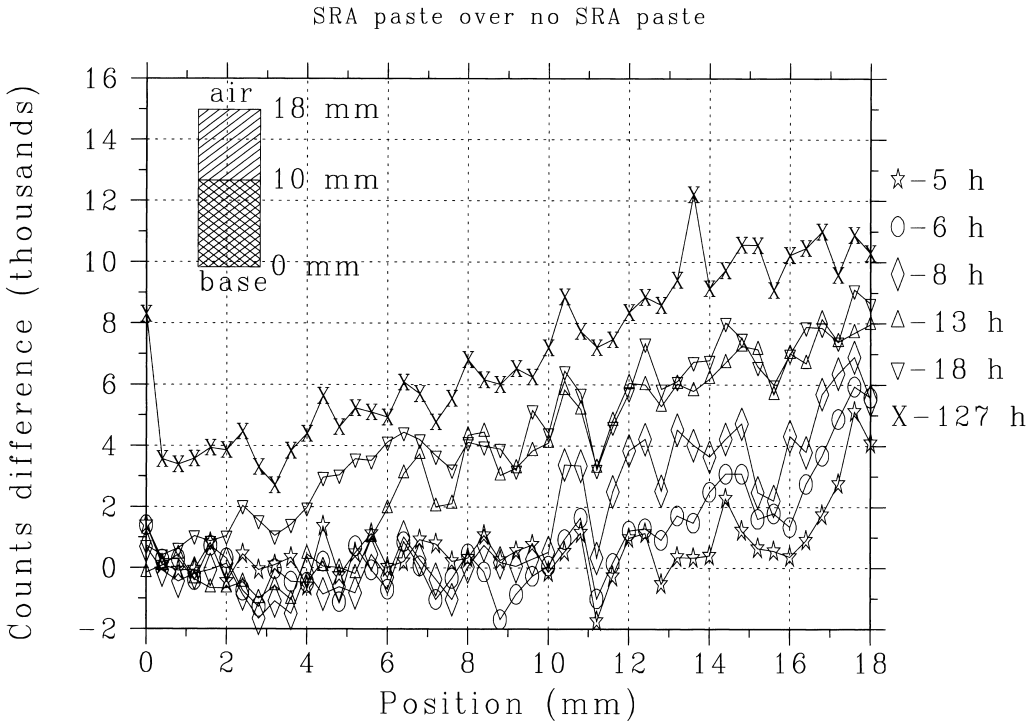

Fig. 7. Differences in normalized X-ray counts vs. position for cement paste with the SRA on top of paste without the SRA. Differences are relative to readings at 4 h.

Because water is maintained at the top surface of the composite specimen for a longer time than in the case where the paste with the SRA is on top, the constant rate drying period is maintained for a longer time and this specimen loses much more water than the one where the layers are reversed (see Fig. 2).

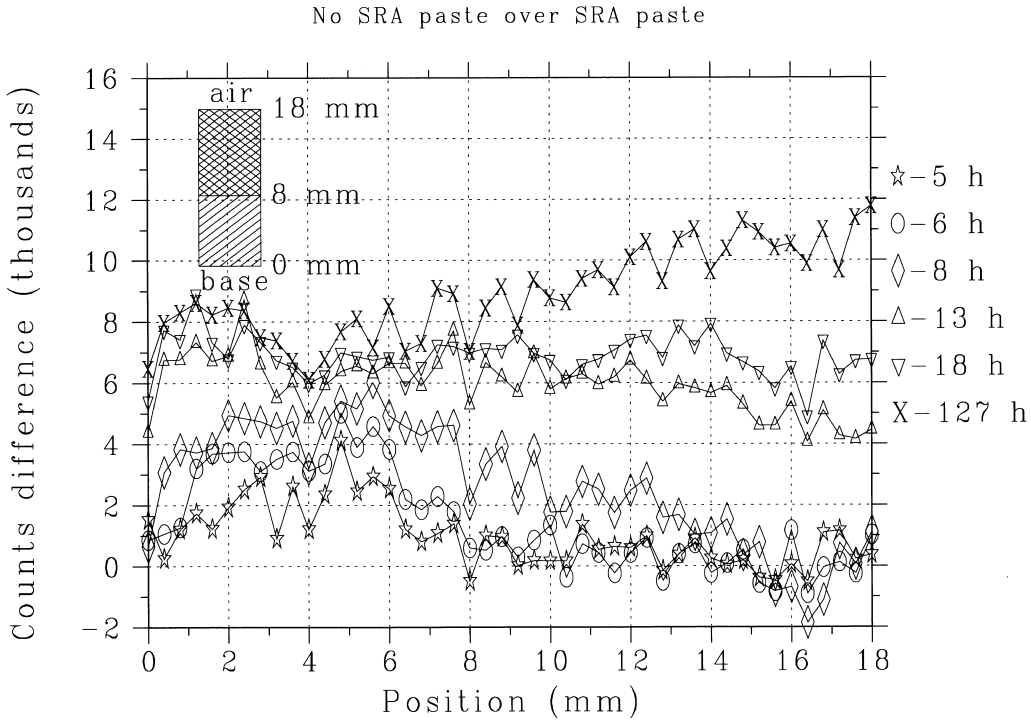

Fig. 8. Differences in normalized X-ray counts vs. position for cement paste without the SRA on top of paste with the SRA. Differences are relative to readings at 4 h.

Further studies were conducted with the SRA for systems cured under sealed conditions. To first verify that the SRA might influence internal RH development and autogenous deformation for specimens cured under sealed curing, the cement pastes prepared with the ultrafine cement (w/c = 0.3) were examined; fine cements with a low w/c ratio tend to maximize the observed internal RH reduction [13]. Fig. 9 presents the internal RH development over the course of 11 days for pastes prepared with and without a 2% SRA addition. For ages beyond 1 day, the RH within the paste with the SRA is seen to be higher than that in the paste with no SRA. At earlier times, the SRA actually slightly decreases the RH, most likely due to a dilution effect (Raoult's law [10]). If it assumed that the pore structure in the two cement pastes is basically the same, the differences in RH can be related to differences in surface tension via the Kelvin equation (Eq. (1)) [10]:

$$\ln(\mathrm{RH}) = \frac{-2\gamma V_m}{rRT} \quad (1)$$

where γ is the surface tension of the pore solution in newtons per meter, V_m is its molar volume in cubic meters per mole, r is the pore radius of the largest water-filled pore in meters, R is the universal gas constant (8.314 J/mol·K), and T is the temperature in kelvin. Using this equation, an acceptable prediction (shown in Fig. 9) of the results for the system with the SRA was produced when it was assumed that initially the surface tension of the cement paste pore solution in the system with the SRA was 74% of that of the paste without the SRA and that the SRA is totally absorbed by the hydration products by 400 h of hydration (with a linear absorption rate during this 400 h). Certainly, these assumptions need to be verified in future studies, but suffice it to say that the SRA definitely affects the internal RH development in pastes cured under sealed conditions. Because the RH is linked to the stresses created within the microstructure, this also means that the SRA should influence autogenous shrinkage and early-age cracking. Examining this hypothesis comprised the last portion of the experimental program. In addition to the RH measurements, after the 264 h (11 days) of hydration, the specimens were analyzed to determine their nonevaporable water content. For the specimens without the SRA, a nonevaporable water content of 0.126 g H_2O/g cement (standard deviation of 0.001) was determined. For the specimens containing the SRA, after correcting for the 0.02 mass fraction of SRA, a value of 0.125 g H_2O/g cement (standard deviation of 0.001) was measured. According to these results, the SRA has no effect on the achieved degree of hydration for these cement paste specimens cured under sealed conditions for 11 days.

The final portion of the study considered the early-age properties of mortars prepared with and without the SRA. Here, a base system with a w/s ratio of 0.35 containing 8%

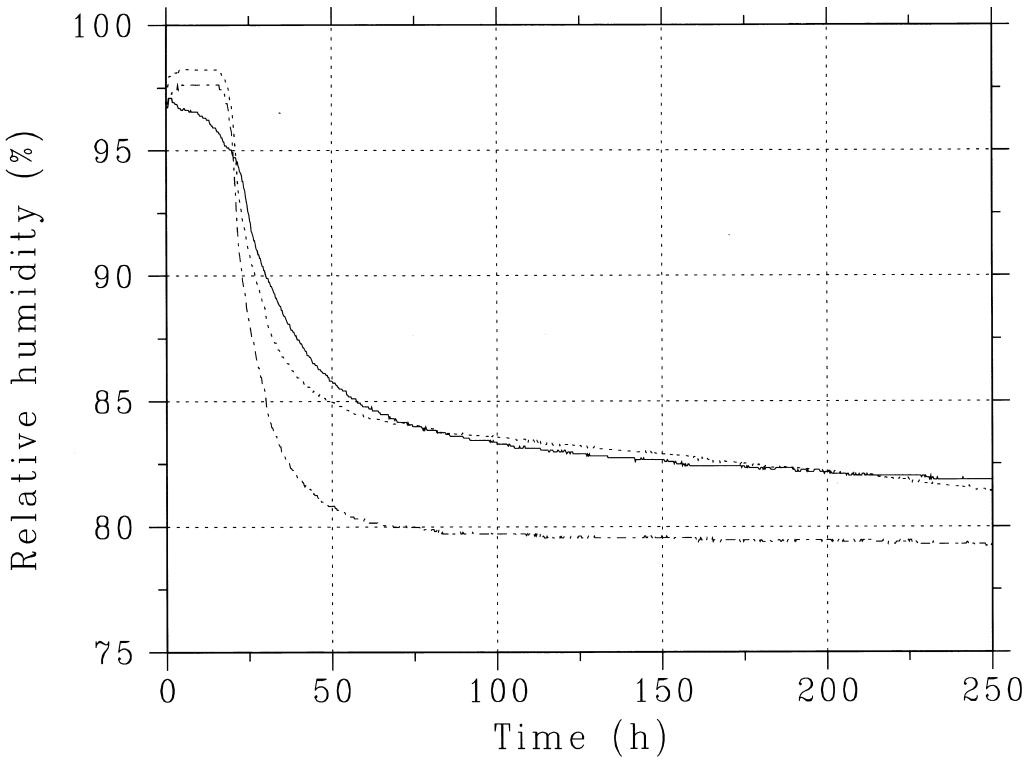

Fig. 9. Differences in internal RH development for cement pastes (w/c = 0.3) with and without the SRA cured under sealed conditions at 25°C. Dashed line is experimental data for the system with no SRA, solid line is experimental data for the system with the SRA, and dotted line is the predicted result for the system with the SRA.

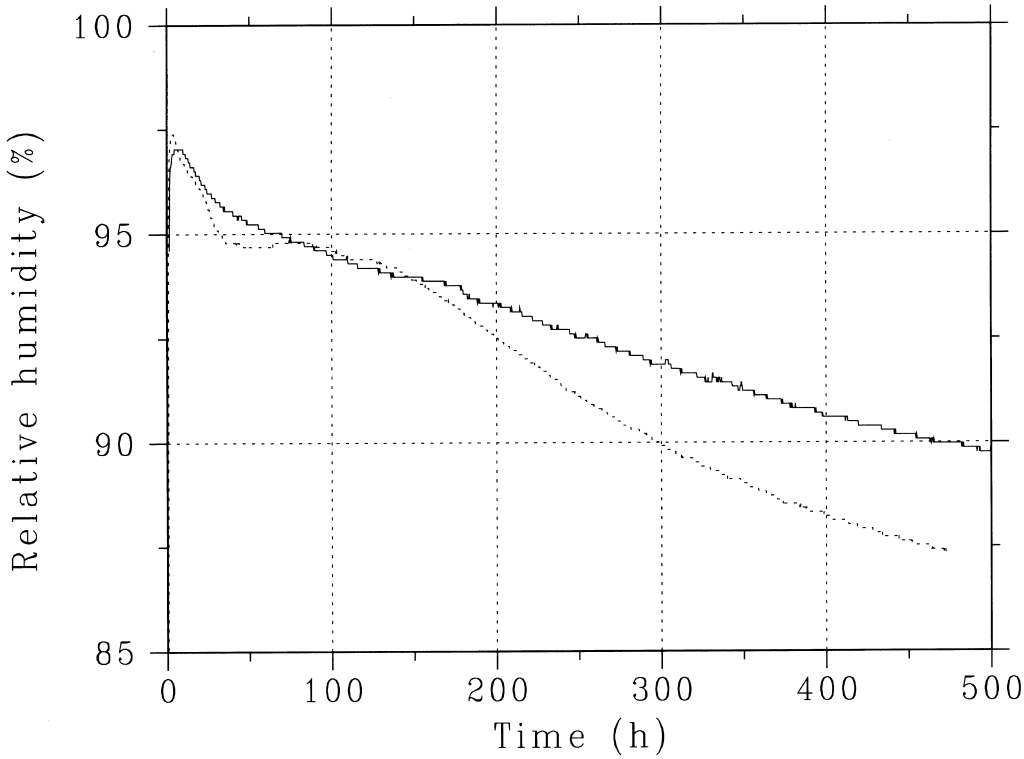

Fig. 10. Differences in internal RH development for cement mortars (w/s = 0.35) with (···) and without (- - -) the SRA cured under sealed conditions at 30°C.

silica fume was used to provide a system where the autogenous shrinkage is significant. This base system can be contrasted against the same mixture containing 2% of the SRA to see if the autogenous shrinkage is indeed reduced. The measured results for these two systems for internal RH and autogenous deformation are provided in Figs. 10 and 11,

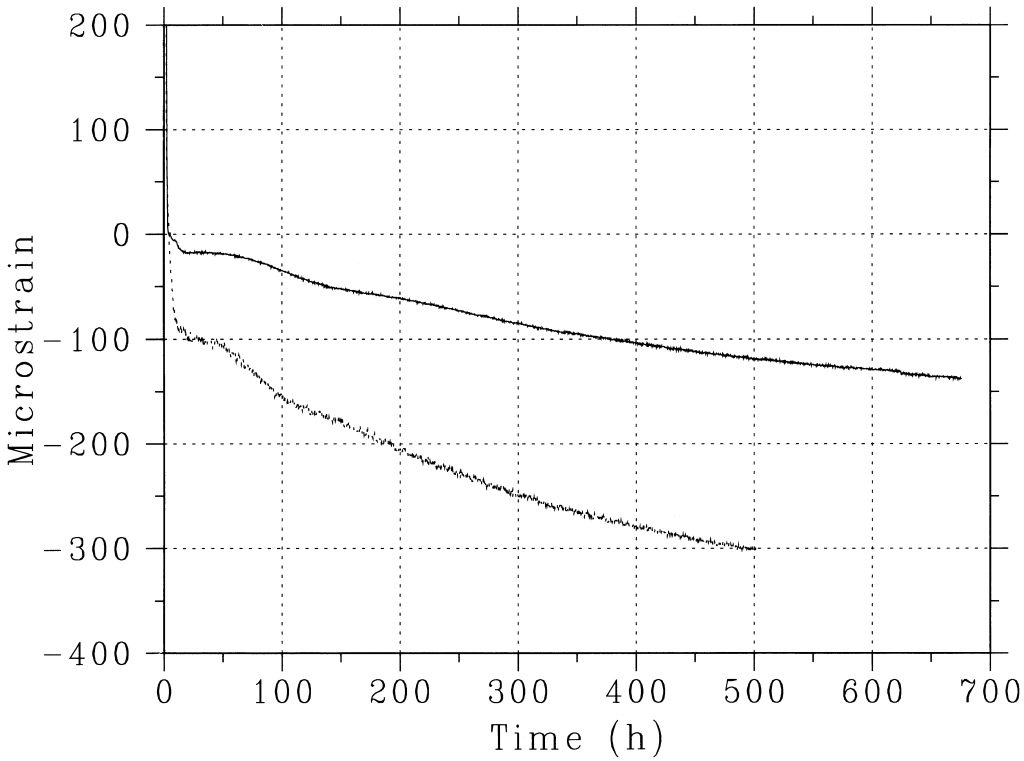

Fig. 11. Differences in autogenous deformation for cement mortars (w/s = 0.35) with (···) and without (- - -) the SRA cured under sealed conditions at 30°C.

respectively. The presence of the SRA is seen to substantially decrease both the reduction in RH and the measured autogenous shrinkage. During the first 3 days or so, the RH in the system with the SRA is substantially higher than that in the system with no SRA. This translates into a system that undergoes almost no autogenous shrinkage during the same time period. After this, the two RH curves approach one another, and then as the silica fume reaction accelerates, they diverge once more. Even as the pore size within the hydrating cement/silica fume paste continues to be reduced, the presence of the SRA continues to result in a substantially higher RH and less autogenous shrinkage. In the long term, the SRA reduces the autogenous shrinkage by more than a factor of two, which should translate to a lower susceptibility to early-age cracking for the mortar containing the SRA. Particularly, the reduction observed during the first 100 h is critical, as it is during this period that the hydrating cement paste is weakest and most susceptible to cracking.

The compressive strengths of mortar cylinders (60 mm in diameter and 120 mm in height) with and without the SRA, cured under sealed conditions at 30°C, were also measured. In each case, three replicates were tested for each mixture and curing age. At 7 days, compressive strengths of 47.9 MPa (standard deviation of 7.0 MPa) and 56.8 MPa (standard deviation of 6.6 MPa) were measured for the systems with and without the SRA, respectively. At 28 days, the strengths were 70.4 MPa (standard deviation of 5.5 MPa) and 61.3 MPa (standard deviation of 7.0 MPa) for the systems with and without the SRA, respectively. Thus, while there seems to be some early-age strength loss due to the SRA, after 28 days of sealed curing, it actually appears to increase the compressive strength of these low w/s ratio mortars containing silica fume. However, considering the standard deviations achieved in the strength testing, these differences are not statistically significant, but the results do indicate that the SRA is not detrimental to 28-day strength for these particular mortars. Conversely, for concretes with w/c = 0.42 and cured at 100% RH, Brooks and Jiang [14] have observed approximately a 28% reduction in 28-day compressive strength for specimens with an SRA (1.5% by mass of cement addition) vs. control specimens prepared without the SRA. For concretes with and without silica fume and a w/s ratio of 0.35, Folliard and Berke [15] observed a 6% to 8% reduction in 28-day strength for specimens containing a 1.5% addition of the SRA, cured at 20°C and 100% RH. In the present study, the use of sealed curing at 30°C (along with the low w/s ratio and the addition of silica fume) is the most likely reason for the apparent strength enhancement produced in the specimens with the SRA. For example, it could well be that the maintenance of a higher internal RH, due to the presence of the SRA, extends the period of time during which the silica fume reacts pozzolanically with the calcium hydroxide formed from the cement hydration, leading to higher degrees of reaction and higher strengths.

4. Conclusions

The addition of an organic SRA was observed to have the following effects in the present experiments:

1. a significant reduction in the surface tension of a solution containing the SRA relative to distilled water,
2. a concurrent increase in the drying rate of bulk solutions,
3. a change in the drying profile from uniform drying to a sharp drying front for w/c = 0.35 cement pastes exposed to drying conditions,
4. a concurrent *decrease* in the drying rate of cement pastes,
5. no influence on the achieved degree of hydration for cement pastes cured under sealed conditions for 11 days,
6. a decrease in the internal RH reduction in low w/c ratio cement pastes and mortars cured under sealed conditions,
7. a significant decrease in autogenous shrinkage in low w/c ratio mortars cured under sealed conditions, and
8. no significant change in 28 day compressive strength for w/s = 0.35 (8% silica fume) mortar cylinders cured under sealed conditions at 30°C.

These results will have implications for the mitigation of early-age cracking in low w/c ratio concretes and also possibly for the design of improved curing systems and methodologies.

Acknowledgments

This research was performed while the first author was a visiting professor at the Technical University of Denmark, funded by the Knud Hojgaard Foundation. The provision of materials by Aalborg Portland Cement, Dyckerhoff Zement, and W.R. Grace & Co.-Conn. is gratefully acknowledged. Useful discussions with Prof. Ole M. Jensen of Aalborg University are also gratefully acknowledged.

References

[1] J.F. Lawless, Statistical Models and Methods for Lifetime Data, Wiley, New York, 1982.
[2] H.F.W. Taylor, Cement Chemistry, 2nd ed., Thomas Telford, London, 1997.
[3] T. Sato, T. Goto, K. Sakai, Mechanism for reducing drying shrinkage of hardened cement by organic additives, CAJ Rev. (1983) 52–54.
[4] K.K. Hansen, S.K. Jensen, L. Gerward, K. Singh, Dual-energy X-ray absorptiometry for the simultaneous determination of density and moisture content in porous structural materials, Proc. 5th Symp. Build. Phys. Nordic Countries, Gothenburg, Sweden, 1999, vol. 1, pp. 281–288.
[5] D.P. Bentz, K.K. Hansen, Preliminary observations of water move-

ment in cement pastes during curing using X-ray absorption, Cem. Concr. Res. 30 (2000) 1157–1168.
[6] D.P. Bentz, K.K. Hansen, H.D. Madsen, F. Valle, E.J. Griesel, Drying/hydration in cement pastes during curing, Mater. Struct. (accepted for publication).
[7] O.M. Jensen, P.F. Hansen, Autogenous relative humidity change in silica fume modified cement paste, Adv. Cem. Res. 7 (25) (1995) 33–38.
[8] O.M. Jensen, P.F. Hansen, A dilatometer for measuring autogenous deformation in hardening Portland cement paste, Mater. Struct. 28 (1995) 406–409.
[9] O.M. Jensen, P.F. Hansen, Autogenous deformation and change of relative humidity in silica fume modified cement paste, ACI Mater. J. 93 (6) (1996) 539–543.
[10] R.A. Alberty, F. Daniels, Physical Chemistry, Wiley, New York, 1980.
[11] D.P. Bentz, D.A. Quenard, V. Baroghel-Bouny, E.J. Garboczi, H.M. Jennings, Modelling drying shrinkage of cement paste and mortar: Part 1. Structural models from nanometers to millimeters, Mater. Struct. 28 (1995) 450–458.
[12] P. Coussot, Scaling approach of the convective drying of a porous medium, Eur. Phys. J. B 15 (2000) 557–566.
[13] D.P. Bentz, O.M. Jensen, K.K. Hansen, J.F. Olesen, H. Stang, C.J. Haecker, Influence of cement particle size distribution on early age autogenous strains and stresses in cement-based materials, J. Am. Ceram. Soc. 84 (1) (2001) 129–135.
[14] J.J. Brooks, X. Jiang, The influence of chemical admixtures on restrained drying shrinkage of concrete, in: V.M. Malhotra (Ed.), Superplasticizers and Other Chemical Admixtures in Concrete, Am. Concr. Inst., SP 173 (1997) 249–265.
[15] K.J. Folliard, N.S. Berke, Properties of high-performance concrete containing shrinkage-reducing admixtures, Cem. Concr. Res. 27 (9) (1997) 1357–1364.